Detecting Supernovae Type Ia Progenitors with the Laser Interferometer Space Antenna

Frank Ceballos

July 23, 2012

Abstract

The Galactic population of close white dwarf binaries is expected to provide the largest number of gravitational wave sources for low frequency detectors such as the Laser Interferometer Space Antenna (LISA). We model the current population of close white dwarf binaries in the Galaxy using the population synthesis tool StarTrack and observe with a simulated LISA for a period of two years. From the two-year observation, an appreciable fraction of the 10^4 binaries detected will be progenitors of Type Ia supernovae. We report on the properties of the detected binaries and conclude that if LISA were to be launched it would expand our knowledge about the Galaxy and about Type Ia supernovae.

Contents

1 Introduction

1.1 The Type Ia Supernova

The 2011 Nobel Prize in Physics was awarded to Saul Perlmutter, Brain P. Schmidt, and Adam G. Riess for showing the accelerating expansion of the Universe through observations of Type Ia Supernovae (SNe Ia) in distant galaxies. They measured the SNe Ia light curves, assumed the explosion mechanism was the same for each supernova, and compared the expected redshift light intensity to the observed light intensity. This led them to conclude that the Universe was not only expanding but accelerating [1]. Despite the great importance of SNe Ia, neither the nature of the explosion nor the progenitors of such physical events are well understood. Two main competing progenitor scenarios have been proposed. We briefly discuss the single degenerate (SD) scenario in the next section but only consider the double degenerate (DD) scenario as progenitors of SNe Ia, where the explosion is caused by the merging of two carbon-oxygen white dwarfs, with a combined mass exceding the Chandrasekhar limit, that spiral in due to the emission of gravitational waves [2].

1.2 The Single Degenerate Scenario

The single degenerate (SD) scenario refers to the case where a carbon-oxygen white dwarf (WD) accretes matter from a non-degenerate companion (either a red giant or sub-giant) that has overfilled it Roche lobe. The WD grows in mass until it reaches the Chandrasekhar mass limit, it then implodes because it is unable sustain itself against the tremendous pressure of gravity. As a result, the core heats up and the CO begins to fuse. The amount of energy released by the fusion of CO is such that the WD explodes, producing a SNe Ia, leaving no remnant behind. One drawback of this scenario is that population synthesis calculations that assume the SD scenario as progenitors of SNe Ia do not agree with observations; specifically the SD rate is an order of magnitude lower than the observed SN Ia rate [3]. More recently observational evidence against the SD scenario has been provided [4]. In the SD scenario, the white dwarf is destroyed during the explosion but the companion remains behind. Edwards, Pagnotta, and Schaefer searched for the companion of the SN Ia that created SNR 0519-69.0 in the large magellanic cloud and concluded that either the progenitor of the SN Ia was either formed by a supersoft source or a double-degenerate since all of the stars nearby where the explosion occurred were main sequence stars.

1.3 On Double White Dwarfs

In 1984 Webbink, seeing that models of the birth rates of Type Ia supernovae by evolution of double white dwarfs agreed with observational estimates, proposed that SNe Ia progenitors may be close double white dwarfs (CDWD). From population synthesis models it is estimated that there exist on the order of 3.0×10^7 or so binary systems consisting of CDWD that emit gravitational waves (GW) in the 10-100 mHz range [5]. Most of them lie in the low frequency range (0.1-3.0 mHz) producing a noise that makes detection of CDWD unlikely at this frequencies. The formation of CDWD arises in systems in which the constituents' zero-age main sequence (ZAMS) masses range from 1-9 $M_\odot$ and have initial separations between 10-1000 $R_\odot$ [6]; the end products fall mainly into three groups: helium/helium, helium/carbon-oxygen, and carbon-oxygen/carbon-oxygen white dwarfs. Due to the emission of gravitational waves, the orbit of the binaries shrinks and ultimately the white dwarfs merge binaries composed of two carbon-oxygen white dwarfs with a total mass exceeding the Chandrasekhar mass are destined to become a SN Ia.

1.4 Formation of CO/CO Pairs

According to Evans [6], if a binary system consists of intermediate-mass components (i.e. its components ZAMS is in the range of 5-9 $M_\odot$) and has an initial separation of order 70-500 $R_\odot$, then the more massive (primary) star will fill its Roche lobe after it finishes burning the hydrogen in its core, but before igniting helium. That is because a heavier star will fuse hydrogen in their core at a higher rate than the less massive star. Consequently, the primary star will finish burning the hydrogen in its core before its less massive companion. Since the core is not hot enough to fuse helium, it is left without an outward pressure to counteract the pressure of gravity, thus it collapses. The temperature of the core rises, causing the outer layers of gas that surround the star to expand and fill its Roche lobe. During this stage the mass transfer proceeds with small losses of mass and angular momentum [2]. If the mass transfer is extremely rapid, then the accretor will not be able to accrete all the mass. Assuming that angular momentum and energy are conserved, it follows that the separation between the binaries shrinks. As a consequence, the donor will overflow its Roche lobe more which will accelerate mass transfer and more rapidly decrease the separation of the stars. The lost mass that cannot be accreted by the secondary increases its volume causing it to fill the Roche lobe of the secondary; this is known as the common envelope stage. At this stage both stars have overfilled their Roche lobes and are surrounded by the mass lost by the primary star. The mass of the primary is in the range of 0.7 - 1 $M_{\odot}$, which means that common envelope contains most of it, about 4-6 $M_{\odot}$.

As the stars go around their orbits they will experience a drag force exerted by the gas that envelopes them. Therefore, the kinetic energy of each star transfers to the surrounding envelope. Consequently, as the gas heats up the orbits decrease. The hotter gas is less tightly bound to the binary systems and eventually it will become hot enough that it will be completely removed. The energy required to lift off the envelope will shrink the orbit of the helium core and the companion within 10 - 70 $R_{\odot}$ [6] . Once the helium core is hot enough, helium burning will commence and will convert the primary remnant to a degenerate CO dwarf with a mass of 0.7 - 1.0 $M_{\odot}$ in about 10^5yr. When the secondary overfills its Roche lobe, a second common envelope may be formed. The evolution of the common envelope proceeds in a similar manner, which reduces the separation to about 0.2 - 1.4 $R_{\odot}$; helium burning converts the secondary into a CO dwarf.

1.5 Population Synthesis

We populate the Galaxy with WD binaries using the population synthesis tool StarTrack, written by K. Belczynski [7]. His code describes single stellar evolution and the physical interactions of two stars in a binary and further evolves compact stellar remnants formed such as, WD, neutron stars, and black holes. Since we lack knowledge of the physics behind many astrophysical processes, population synthesis may depend on ~30 parameters which some consider to be a major weakness. One of it strengths is that it allows us to approach problems where we lack the full physical picture. Predictions made by population synthesis are then compared to observations that either support or rule out models that attempt to describe physical phenomena, delivering valuable insights.

1.6 Gravitational Waves

Gravitational waves are ripples in space-time predicted by Albert Einstein in 1916. Proof of their existence has been indirectly shown by a close binary system of pulsars (B1913+16). Weisberg & Taylor [8] showed that the rate of change of the orbital period of B1913+16 agrees with the expected change cause by the emission of gravitational waves within 0.2 %.

1.7 LISA

The Laser Interferometer Space Antenna (LISA) is an effort by the European Space Agency to measure gravitational waves. It will operate by measuring the distance traveled by identical light beams along two adjoining arms of the three spacecraft separated by 5 million kilometers, flying along Earth's orbit around the sun. If a gravitational wave is present it will contract or enlarge the path traveled by the light and by doing so produce a phase difference between the light beams.

2 The LISA Simulation

2.1 General Descripition

The LISA mission is composed of three spacecraft, which will be placed at vertices of an equilateral triangle, that will orbit the sun. The center of mass of the triangle formed by the spacecraft follows a circular orbit at 1 AU, with an orbital period of one year. Apart from orbiting the sun, the triangular formation rotates about its center of mass in a clockwise direction as viewed from the sun. The arm lengths are approximately 5 million km. The goal of the mission is to detect gravitational waves by measuring the difference in the roundtrip distance traveled between two laser beams that fly along adjacent arms of LISA. When a GW passes through the detector it is theorized that it will contract and expand the distance traveled by the laser beams causing a phase difference between them relative to the reference beam. It is this phase difference that LISA will measure. Placing LISA in space does not free it from noise; random forces would produce vibrations on the spacecrafts and the fact that LISA is a 5 million km interferometer means that a small number of photons will be reaching the detector introducing variations in the beam intensity, known as shot noise. Furthermore, the large number of white dwarf binaries in the Galaxy will produce a GW background known as confusion noise; most of them lie in the frequency range of 0.1 - 3.0 mHz, which makes it a more difficult task to resolve GW sources at these frequencies.

2.2 Gravitational Wave Produced by A Binary System

Let us consider a plane polarized GW produced by a binary. To do so we will consider a coordinate system where the binary system lies in the $X' - Y'$ plane and the angular momentum of the binary points in the $\hat{L}$ direction.

The angle the Z' axis makes with $\hat{L}$ is θ'. This signal is more easily described with the use of the transverse-traceless gauge

$$h_{\alpha\beta} = \begin{pmatrix} 0 & 0 & 0 & 0 \\ 0 & h_+ & h_\times & 0 \\ 0 & h_\times & -h_+ & 0 \\ 0 & 0 & 0 & 0 \end{pmatrix}$$

where [5]

$$h_+ = \frac{G^{5/3}}{c^4 d} M_c^{5/3} f^{2/3} (1 + \cos^2 i) \tag{1}$$

$$h_\times = -2 \frac{G^{5/3}}{c^4 d} M_c^{5/3} f^{2/3} \cos^2 i, \tag{2}$$

where d is the distance to the binary, i is the inclination angle, and M_c is known as the chirp mass and is defined as

$$M_c = \frac{(M_1 M_2)^{3/5}}{(M_1 + M_2)^{1/5}}. \tag{3}$$

2.3 Gravitational Wave Strain On LISA Produced by A Binary System

In the absence of a GW, the distance between two points is described by the flat-space metric

$$\eta_{\alpha\beta} = \begin{pmatrix} -1 & 0 & 0 & 0 \\ 0 & 1 & 0 & 0 \\ 0 & 0 & 1 & 0 \\ 0 & 0 & 0 & 1 \end{pmatrix}$$

The presence of a GW will perturb the flat-space metric producing the new metric

$$g_{\alpha\beta} = \eta_{\alpha\beta} + h_{\alpha\beta} \tag{4}$$

where $h_{\alpha\beta}$ is the strain produced by a GW. We use a barycentric coordinate system, where the sun lies in the origin, the X-axis points toward the center of mass of LISA, the Y-axis in the direction perpendicular to X-axis, and the Z-axis is defined by the direction of the ecliptic pole to measure the distance between two spacecrafts in the presence of a GW. Using the transverse-traceless gauge to describe a plane gravitational wave propagating in the $\hat{n}$

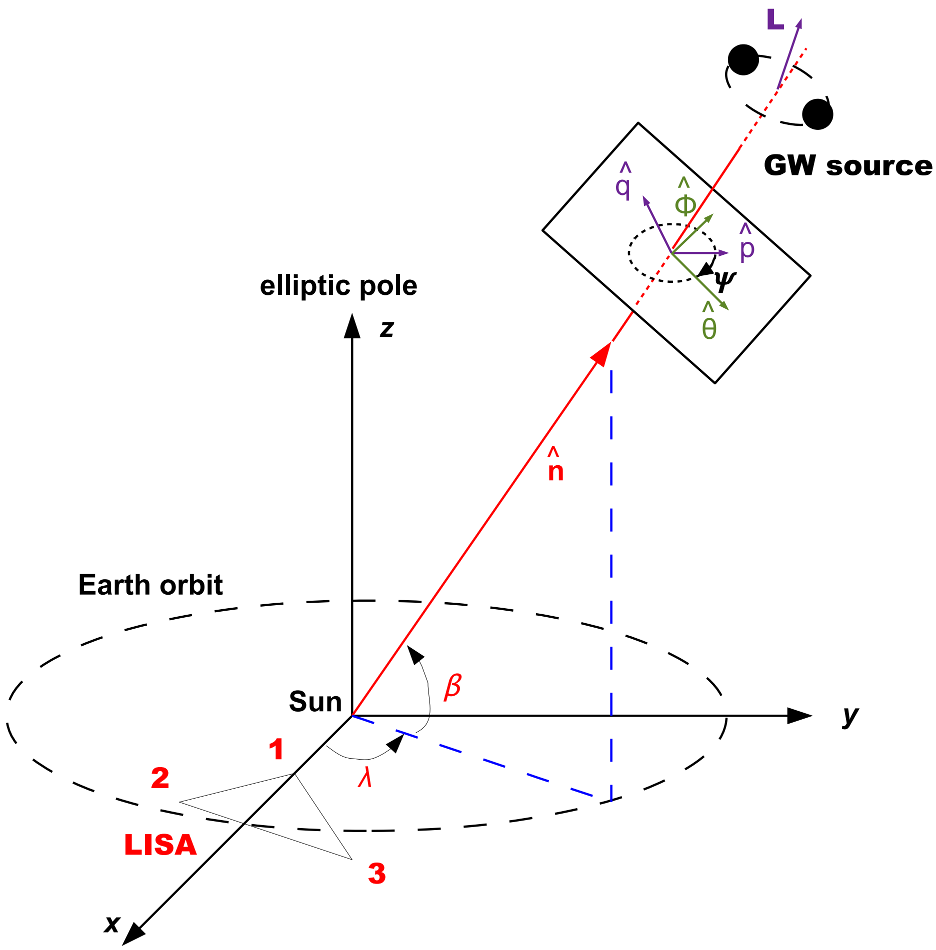

Figure 1: Schematic description of LISA

direction we consider the strain caused in one of LISA's arms. The length L is

$$L = \int_0^{L_0} \sqrt{ds^2}. \tag{5}$$

Next we consider the infinitesimal distance to be $ds^2 = g_{\alpha\beta} dx^\alpha dx^\beta$ and let $x^\alpha = x(\lambda)$ which yields

$$dx^\alpha = \frac{\partial x^\alpha}{\partial \lambda} d\lambda. \tag{6}$$

Substituting this result into 9 gives us

$$L = \int_0^{L_0} \sqrt{\eta_{\alpha\beta} \frac{\partial x^\alpha}{\partial \lambda} \frac{\partial x^\beta}{\partial \lambda} d^2\lambda + h_{\alpha\beta} \frac{\partial x^\alpha}{\partial \lambda} \frac{\partial x^\beta}{\partial \lambda} d^2\lambda} \tag{7}$$

$$L \approx \int_0^{L_0} \sqrt{\eta_{\alpha\beta} \frac{\partial x^\alpha}{\partial \lambda} \frac{\partial x^\beta}{\partial \lambda}} \left(1 + \frac{1}{2} \frac{h_{\epsilon\zeta} \frac{\partial x^\epsilon}{\partial \lambda} \frac{\partial x^\zeta}{\partial \lambda}}{\delta_{\gamma\kappa} \frac{\partial x^\gamma}{\partial \lambda} \frac{\partial x^\kappa}{\partial \lambda}}\right) d\lambda, \tag{8}$$

the perturbation $h_{\alpha\beta}$ is taken to small which allows us to make a first order approximation. To evaluate integral we introduce the following substitutions [9]:

$$x^\alpha = \lambda \ell^\alpha \tag{9}$$

$$1 = \ell^\alpha \ell^\beta \eta_{\alpha\beta} \tag{10}$$

where ℓ^α and ℓ^β are units vectors that point along the arms of LISA. With this substitution the integral simply becomes

$$L \approx \int_0^{L_0} \left(1 + \frac{1}{2} h_{\epsilon\zeta} \ell^\epsilon \ell^\zeta\right) d\lambda. \tag{11}$$

Since the wavelength of the GW is much longer than the arm length of LISA, $h_{\epsilon\zeta}$ remains constant along the path. The integral then becomes

$$L \approx \int_0^{L_0} \left(1 + \frac{1}{2} h_{\epsilon\zeta} \ell^\epsilon \ell^\zeta\right) d\lambda = L_0 \left(1 + \frac{1}{2} h_{\epsilon\zeta} \ell^\epsilon \ell^\zeta\right), \tag{12}$$

where L_0 is the arm length of the interferometer. We define the relative difference between two adjacent arms to be

$$h(t) = \frac{1}{2} h_{\alpha\beta} (\hat{l_1}^\alpha \hat{l_1}^\beta - \hat{l_2}^\alpha \hat{l_2}^\beta). \tag{13}$$

The response of a noise free detector to a GW source will be $S(t) = h(t)$, where $h(t)$ is the strain a GW would produce.

2.4 Acceleration Noise, Shot Noise, Position Noise, and Confusion Noise

Two major noise contributions in the instrument are due to stochastic processes, these are known as acceleration noise and shot noise. The acceleration noise is the product of the random forces that the test masses experienced in their roundtrip orbit around the sun. The shot noise is the effect of the low number of photons reaching the the detectors at random times. Thus we model the acceleration noise and the shot noise on each spacecraft by drawing values randomly from independent Gaussian distributions on the frequency domain, multiplying it by the one sided spectral density, either by $S_s(f)^{1/2} = 20 \times 10^{-12}$ mHz$^{-1/2}$ (for the shot noise) or $S_a(f)^{1/2} = 3 \times 10^{-15}[1 + (10^{-4}\ \mathrm{Hz}/f)^2]^{1/2}$ ms^{-2} Hz$^{-1/2}$ (for the acceleration noise), and fast Fourier transform (FFT) into the time domain [10]. Because we do not know where exactly the spacecraft will be located at any given point in time another type of noise is introduced into LISA, denoted as position noise. We generate the position noise from the acceleration noise by integrating it twice in the Fourier domain which introduces a factor of $(i\omega)^{-2}$ and inverse Fourier transform it to the time domain. Finally, the the power spectral density of the confusion noise produced by the white dwarf binaries is [11].

$$n(f) = \begin{cases} 1.65 \times 10^{-39}(\frac{f}{1.0\times10^{-4}})^{0.2099} : f \in (1.0 \times 10^{-4}Hz,\ 2.5 \times 10^{-4}Hz] \\ 2.0 \times 10^{-39}(\frac{f}{2.5\times10^{-4}})^{-0.4894} : f \in (2.5 \times 10^{-4}Hz,\ 4.5 \times 10^{-4}Hz] \\ 1.5 \times 10^{-39}(\frac{f}{4.5\times10^{-4}})^{-0.9545} : f \in (4.5 \times 10^{-4}Hz,\ 1.0 \times 10^{-3}Hz] \\ 7.0 \times 10^{-40}(\frac{f}{1.0\times10^{-3}})^{-1.7095} : f \in (1.0 \times 10^{-3}Hz,\ 1.5 \times 10^{-3}Hz] \\ 3.5 \times 10^{-40}(\frac{f}{1.5\times10^{-3}})^{-2.9453} : f \in (1.4 \times 10^{-3}Hz,\ 2.0 \times 10^{-3}Hz] \\ 1.5 \times 10^{-40}(\frac{f}{2.0\times10^{-3}})^{-5.1290} : f \in (2.0 \times 10^{-3}Hz,\ 2.2 \times 10^{-3}Hz] \\ 9.2 \times 10^{-41}(\frac{f}{2.2\times10^{-3}})^{-18.1819} : f \in (2.2 \times 10^{-3}Hz,\ 2.3 \times 10^{-3}Hz] \\ 4.1 \times 10^{-41}(\frac{f}{2.3\times10^{-3}})^{-18.0531} : f \in (2.3 \times 10^{-3}Hz,\ 2.5 \times 10^{-3}Hz] \\ 9.1 \times 10^{-42}(\frac{f}{2.5\times10^{-3}})^{-15.391} : f > 2.5 \times 10^{-3}Hz \end{cases}$$

At the end the signal detected by LISA is

$$S = S_a + S_p + S_s + n_b + h(t), \tag{14}$$

where S_a is the signal produced by the acceleration noise, S_s is the signal produced by the shot noise, S_p is the signal produced by the position noise, n_b is the signal produced by the confusion noise, and $h(t)$ is the gravitational wave strain on LISA.

3 Data Analysis

3.1 Overview

We compute the LISA response to the entire population over a two-year observation time. In order to reduce computational time, in searching for all the 30 million binaries in the data stream recorded by LISA, we compute the signal to noise ratio for all 30 million binaries (explained in the following section) and select only those double white dwarf binaries with a signal to noise ratio (ρ) greater or equal to five. Binaries that pass the threshold test are then run through the data analysis pipeline described in the Match section.

3.2 SNR

The signal-to-noise ratio is defined as

$$\rho^2 = 4\int_0^\infty \frac{\left|\tilde{h}(f)\right|^2}{S_n(f)} df \tag{15}$$

where $S_n(f)$ is the one sided spectral density of the noise in LISA and $\tilde{h}(f)$ is the Fourier transform of the signal produce by a binary.

Next, we take advantage of the nature of a gravitational wave produced by a white dwarf binary. Most of the power in the gravitational wave will be distributed at a specific frequency f_0 which can be more explicitly stated as

$$\tilde{h}(f) = A\delta(f - f_0). \tag{16}$$

We substitute this form of $\tilde{h}(f)$ into the definition of the signal-to-noise ratio to obtain

$$\rho^2 = 4\int_0^\infty \frac{A^2\delta(f - f_0)}{S_n(f)} df. \tag{17}$$

As a result, the $\delta(f - f_0)$ in the integrand evaluates the integral to be

$$\rho^2 = \frac{4A^2}{S_n(f_0)}, \tag{18}$$

where A is the amplitude of the GW produce by a binary given by [12]

$$A = \frac{2(GM_c)^{\frac{5}{3}}}{c^4 d}\left(\frac{\pi}{P_{GW}}\right)^{2/3}. \tag{19}$$

In equation (19), G is Newton's gravitational constant, d is the distance to the binary, M_c is the chirp mass, and P_{GW} is the period of the gravitational wave. For binaries with circular orbits the gravitational wave period P_{GW} and the orbital period of the binary P_{orb} are simply related by a factor of 2. That is

$$P_{\mathrm{orb}}(t) = 2P_{\mathrm{GW}}(t) \tag{20}$$

and

$$P_{\mathrm{orb}}(t) = \left(P_0^{8/3} - \frac{8}{3}kt\right)^{3/8}, \tag{21}$$

where P_0 is the orbital period at $t = 0$ and k is a constant given by

$$k \equiv \frac{96}{5c^5}(2\pi)^{8/3}(GM_c)^{5/3}. \tag{22}$$

3.3 Match

Binaries that pass the signal-to-noise ratio threshold are searched for in the data stream—but not blindly. We define χ^2 to be

$$\chi^2 = \frac{1}{N}\sum_i^N \frac{(D_i - M_i)^2}{\sigma_N^2} \tag{23}$$

where D_i is the data stream recorded by LISA, M_i is our model (in this case the waveform computed using the 8 known parameters of the binary), and σ_N is the standard deviation of the noise. To see how χ^2 works, let

$$D_i = S_i + n_i \tag{24}$$

where S_i is the actual signal from a binary and n_i is simply random noise. Making this substitution into the definition of χ^2 and expanding the numerator we obtain

$$\chi^2 = \frac{1}{N}\sum_i^N \frac{S_i^2 + n_i^2 + 2S_i n_i - 2S_i M_i - 2n_i M_i + M_i^2}{\sigma_N^2}. \tag{25}$$

Since the noise is random the terms multiplied by n_i will average out to zero leaving us with

$$\chi^2 = \frac{1}{N}\sum_{i}^{N}\frac{(S_i - M_i)^2 + n_i^2}{\sigma_N^2}. \tag{26}$$

The result shows that if our model is the exact signal of the binary, that is

$$M_i = S_i, \tag{27}$$

then

$$\chi^2 = \frac{1}{N}\sum_{i}^{N}\frac{n_i^2}{\sigma_N^2} = 1. \tag{28}$$

Thus values of χ^2 close to one imply that the model M_i is likely to be contained in the data stream, and values of χ^2 greater than one correspond to models M_i that are less likely to be contain in the data stream. Remember that M_i is characterized by 8 different parameters which makes χ^2 a function of 8 parameters. Thus if we want to obtain a good model or fit, χ^2 must be minimize in an eight parameter space. The algorithm we use to optimize χ^2 is known as the Nelder-Mead method [13]. The Nelder-Mead method is a simplex (a generalization of a triangle in n dimensions) method for finding a local minimum of a function. Let $P_0, ..., P_n$ be the vertices of the simplex formed in the n dimensional space and denote the values of χ^2 at a given point P_i as χ_i. We then define

$$\chi^2_{\mathrm{h}} = \max(\chi^2_{\mathrm{i}}) \tag{29}$$

$$\chi^2_{\mathrm{l}} = \min(\chi^2_{\mathrm{i}}). \tag{30}$$

The subscript h indicates the highest value of the set $\{\chi_i^2\}$ and l the lowest value of the set $\{\chi_i^2\}$. We further define the centroid of the simplex as

$$\bar{P} = \sum_{i\neq h}^{n}\frac{P_i}{n} \tag{31}$$

and write the distance between any two given points as $[P_iP_j]$. The worst vertex (where χ^2 is the greatest) is rejected and replaced with a new vertex using the following operations: reflection, contraction, and expansion. At each step, a new simplex is formed and χ^2 is evaluated at each vertex; the replacement of the worst vertex continues until the parameters that optimize χ^2 are found. Once the worst vertex is found it is reflected as follows

$$P_* = (1+\alpha)\bar{P} - \alpha P_{\mathrm{h}}, \tag{32}$$

where α is a positive constant known as the reflection coefficient. Whenever χ^2_* is between $[y_l, y_h]$, we replace P_h by P_* and restart again with the newly formed simplex. In the case that $\chi^2_* < \chi^2_\mathrm{l}$, it appears that a step into right direction of the minimum has been taken. It only seems natural to stretch further into this same direction therefore we expand by forming a new vertex at

$$P_{**} = \gamma P_* + (1-\gamma)\bar{P}. \tag{33}$$

Gamma is known as the expansion coefficient and is defined as the ratio between $[P^{**}\bar{P}]$ to $[P^*\bar{P}]$. Consequently, gamma is greater than one. With the condition that the new expanded vertex gives the result of $\chi^2{**} < \chi^2_\mathrm{l}$, P_h is replaced by P^{**}. But if $\chi^2{**} > \chi^2_\mathrm{l}$, a step away from the minimum has been taken thus we disregard this expanded vertex and replaced P_h with P_* and restart the process again. In the case that by replacing P_h by P_* leaves $\chi^2_* > \chi^2_i$ for all $i \neq h$, that is if we replace the worst vertex with another worst vertex, we define a new P_h (the vertex P_h or P_* that yields the lowest value of χ^2) and form

$$P_{**} = \beta P_\mathrm{h} + (1-\beta)\bar{P}. \tag{34}$$

β is known as the contraction coefficient, lies between 0 and 1, and is defined as the ratio of $[P^{**}\bar{P}]$ and $[P\bar{P}]$. Provided that $\chi^2_{**} < \min(\chi^2_h, \chi^2_*)$, P_{**} is accepted for P_h, otherwise all the vertices are replaced by

$$P_i' = \frac{P_i + P_\mathrm{l}}{2}. \tag{35}$$

The replacement of the worst vertex is halted when the standard deviation of $\{\chi^2_i\}$ falls below a threshold value. The standard deviation we define as

$$\sigma = \sqrt{\sum_{i=0}^{N} \frac{(\chi^2_i - \bar{\chi}^2)^2}{N}} \tag{36}$$

where N is the number of dimensions. The parameters obtained by the use of the Nelder-Mead method we denote as the recovered parameters. In order to claim that we have detected a binary we make use of cross-correlation (cc), which is a measure of the similarity of two different waveforms. It is defined for two continuous functions f and g as

$$(f \star g)(t) \equiv \int_{-\infty}^{\infty} f^*(\tau) g(t+\tau) d\tau, \tag{37}$$

where f^* is the complex conjugate of f. In order to make this integral evaluate to a number between -1 and 1, a normalization coefficient must be introduced. To grasp a better understanding of the cc, let both f and g be equal to $\cos(\tau)$. Thus we will be integrating $\cos^2(\tau)$ over integral number of periods. This will yield a cc of 1, which means that the functions are identical. So we compute the cc between the recovered waveforms and actual waveforms, and if the cc > 0.9 we claim that we have detected a binary.

4 Results

We model the population of close double white dwarfs (CDWDs) for the bulge and the disk of the Galaxy using the StarTrack population synthesis code of Belczynski [7]. It assumes a constant star formation rate over the past 10 Gyr for the disk and a constant star formation over the first Gyr for the bulge. This produces a population of 27,835,248 CDWDs within the LISA sensitivity band from which 1.45% are potential SN Ia progenitors (405,039). Since most the binaries in this population will be undetectable we restrict our analysis to binaries that have a signal-to-noise ratio that is greater or equal to five. This condition brings the population of CDWD to 39,648 binaries which is 0.14% of the total population and the population of SN Ia progenitors to 653 which 0.16% of the SN Ia progenitors population. This means that 1.64% of the population we will search in the data recorded by LISA will be potential SN Ia progenitors. We run this subset of binaries through the data analysis algorithm (described in the previous section) which is able to resolve 31,169 binaries from the 39,648 binaries that were searched for. Of the 653 potential SN Ia progenitors 503 were resolved, which is 77% of the potential progenitors searched. All of this is summarized in Table 1. Something to note is that the detected number of binaries by LISA is 31,169 and the known number of white dwarf binaries is approximately 1-100. From this we then can conclude that LISA will uncover this hidden population and provide a large enough population of binaries that will allow us to study binary evolution in detail. Furthermore, the current known population SN Ia progenitors is zero. Our result show that LISA will effectively identify such progenitors systems providing once again a population to study the evolution of systems that will produce the essential SN Ia.

4.1 Complete View of the Galaxy

From the resolved binaries we are able to find three important results. First, they show that LISA will be able see through the Galaxy (see figure 2 & 3)

Table 1: The Populations

population	# CDWD	# SN Ia
All	27,835,248	405,039
SNR > 5	39,648	653
Resolved	31,169	503

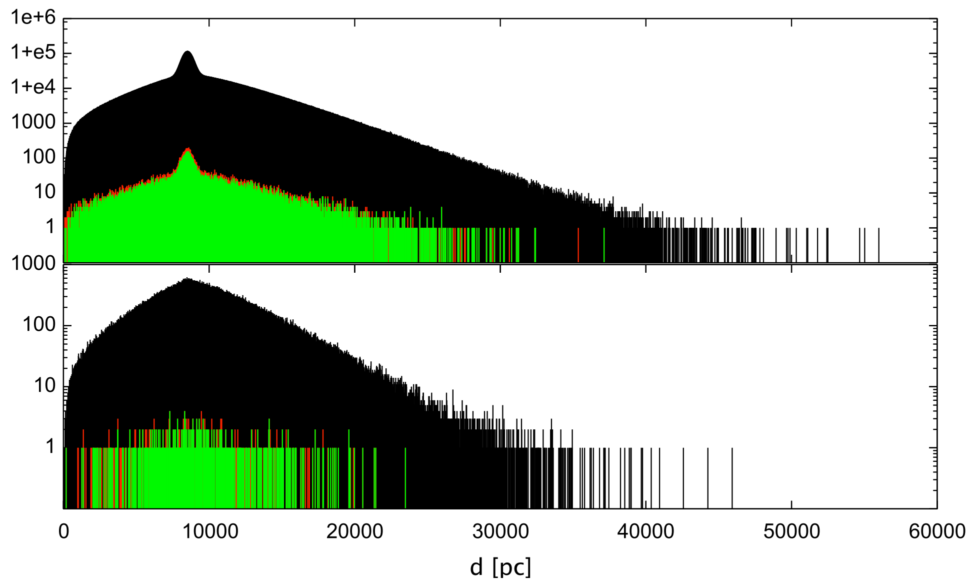

Figure 2: Histograms of distances to the double white dwarfs. The underlying population is in black, the systems with a signal-to-noise ratio greater than 5 are in red, and the resolved systems are shown in green. The center of the Galaxy can be seen at 8.5 Kpc

thus providing for the first time a complete map of the CDWD in the Galaxy. This can be seen in figure 2 which gives histograms of the distances to the binaries. The black histogram shows the underlying population of either the total CDWD binaries (top) or SN Ia progenitors (bottom). The red histogram corresponds to binaries (top) or SN Ia progenitors (bottom) with a signal-to-noise greater or equal to five. The green histogram corresponds to resolved systems. If we examine the top histograms (CDWD) and the bottom histograms (SN Ia progenitors), we can see that even though CDWD concentrate the most in the bulge there are less progenitors of SN Ia in this region. This can be explained by the fact that most stars in the bulge are old hence most progenitors in this region have had enough time to merge. Examination of the resolved system histogram demonstrates that LISA will be able to observe binaries to distances up to 30 kpc. To show how completely and uniformly LISA will see through the Galaxy we plot it the position of the resolved systems shown in figure 3 (viewed from above the Galaxy). The black points represent the resolved binaries by LISA and the red points stand for potential SN Ia progenitors. The approximate position of the sun is shown in cyan.

4.2 No Appreciable Bias On The Detected Population

The second important result that we obtain is that the resolved population is similar to the overall population. That is the detected sample resembles the true sample. This means that LISA will be able to sample evenly, no matter what the actual population of white dwarf is, through the entire population of CDWD. To see this more concretely , figure 4 shows a scatter plot of masses of the binaries. In it you can see the complete population in black, the detected population in red, and the detected SN Ia progenitors in red.

4.3 Visibility of All Binaries With $f > 3$ mHz

The most striking result is that nearly all the binaries we search for with a $f_{\rm GW} > 0.003$ Hz were detected by LISA. Figure 5 shows three stacked histograms of the number of binaries per frequency. In each plot the overall population is represented by the black histogram while SN Ia progenitors are shown on red. The histograms in the top of figure 5 are histograms of the whole population, the histograms in the middle are histograms of binaries with and signal-to-noise ratio greater or equal to five, and the bottom histograms are histograms of the detected binaries by LISA. If you

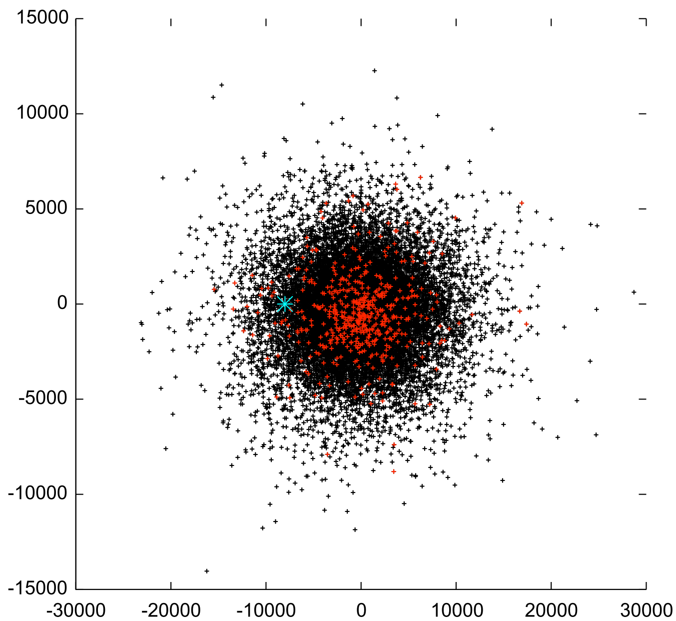

Figure 3: The spatial distribution of the resolved binaries viewed from above the Galaxy. The resolved binaries are shown in black while the potential SNe Ia progenitors are shown in red. The sun is shown in cyan.

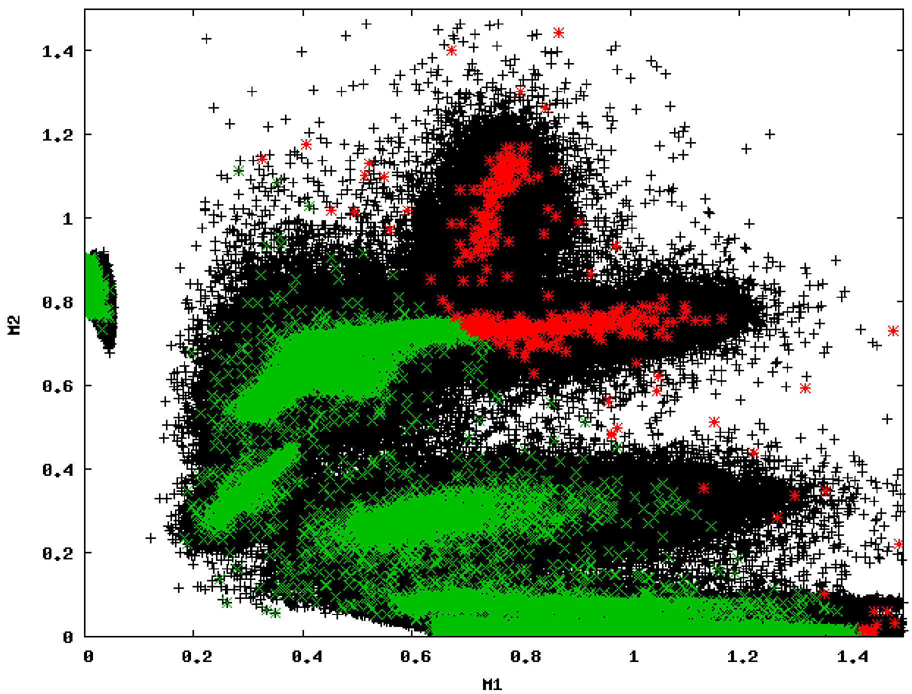

Figure 4: Plot of the masses of the binaries. The total population is shown in black, the detected population in green, and the detected SN Ia progenitors in red.

compare the detected population histograms (BOTTOM) with the total population (TOP) histograms you will observe that they look identical at $f_{\rm GW} > 0.003$ Hz. Such results allows to conclude that LISA will observe the entire population of CDWD binaries with a $f_{\rm GW} > 0.003$ Hz.

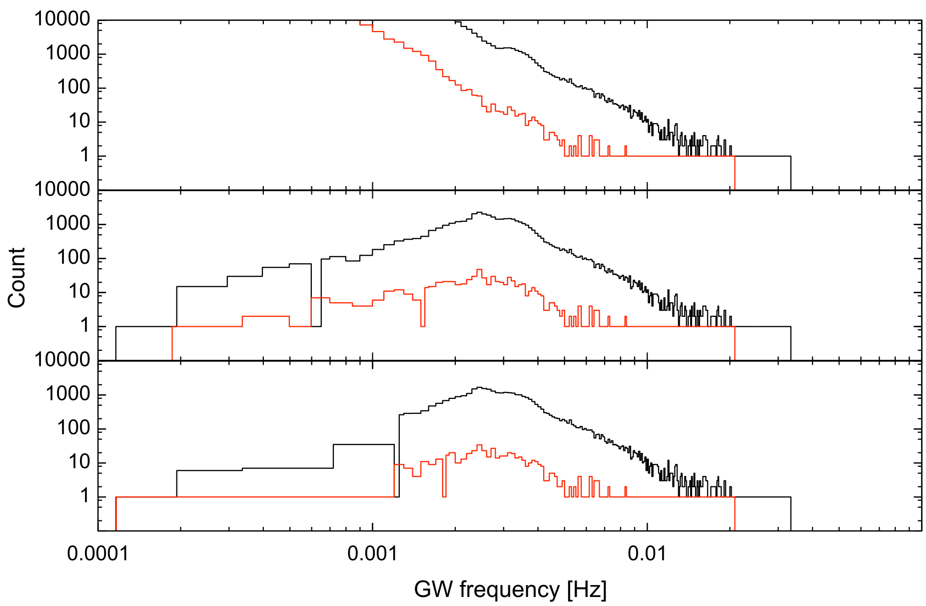

Figure 5: Number in frequency space for the underlying population of double white dwarfs (top panel), for systems with a signal-to-noise ratio greater than 5 (middle panel), and for resolved systems (bottom panel).

5 Conclusions

We have found that LISA will be able to resolve less than 0.1% of the Galactic DWDs within its sensitivity band of f $\geq$ 0.1 mHz. In the underlying population of our synthetic Galaxy, 1.4% of these DWDs are potential SNe Ia progenitors. The resolved population consists of nearly every binary with a gravitational wave frequency above 3 mHz, and that this population is observable throughout the Galaxy. Type Ia progenitors makeup about 1.4% of the resolved systems, and so there are no appreciable biases in this population. Thus, LISA can be considered to be an effective tool for identifying the Galactic population of DWDs and the SNe Ia progenitors within it.

6 Acknowledgment

I am greatly indebted to Matthew Benacquista for providing his enlighten guidance and support throughout these years. I will like to thank Alexander Stroeer for without his great efforts this project will have not been completed and Krzysztof Belczynski for the use of StarTrack results. I am obligated to show gratitude to all members of the ARCC faculty for their distinguish support; specially Dr. Fredrick Jenet for making the ARCC program possible . I thank the Department of Physics & Astronomy at the University of Texas at Brownsville for providing the setting and support that allowed this work to be done. I thank the National Science Foundation for the PAARE grant AST0750913 that supported the ARCC Scholars program, and hence supported my own education and research. I also thank the Center of Gravitational Waves Astronomy at the University of Texas at Brownsville for its support through the NASA URC award NNX09AV06A.

References

[1] G. Brumfiel, Nature **478**, (2011).

[2] R. F. Webbink, The Astrophysical Journal **277**, 355 (1984).

[3] C. L. Fryer *et al.*, The Astrophysical Journal **725**, 296 (2010).

[4] Z. I. Edwards, A. Pagnotta, and B. E. Schaefer, The Astrophysical Journal Letters **747**, L19 (2012).

[5] A. J. Ruiter *et al.*, The Astrophysical Journal **717**, 1006 (2010).

[6] C. R. Evans, I. Iben, Jr., and L. Smarr, The Astrophysical Journal **323**, 129 (1987).

[7] K. Belczynski *et al.*, The Astrophysical Journal Supplement Series **174**, 223 (2008).

[8] J. M. Weisberg and J. H. Taylor, ASP Conf.Ser. **328**, 25 (2005).

[9] L. S. Finn, Phys. Rev. D **79**, 022002 (2009).

[10] in *Laser Interferometer Space Antenna: 6th International LISA Symposium*, Vol. 873 of *American Institute of Physics Conference Series*, edited by S. M. Merkovitz & J. C. Livas (AIP, Melville, New York, 2006), pp. 625–632.

[11] A. Stroeer, Private Communication .

[12] http://cgwp.gravity.psu.edu/outreach/activities/, .

[13] J. A. Nelder and R. Mead, The Computer Journal **7**, 308 (1965).